Non-local Similarity Regularized Sparsity Model for Hyperspectral Target Detection

Zhongwei Huang, Zhenwei Shi and Shuo Yang

Abstract

Sparsity based approaches have been considered useful for target detection in hyperspectral imagery (HSI). Based on the sparse reconstruction theory, the vectors representing spectral signature of hyperspectral pixels can be a linear combination of linearly-dependent training vectors. The training vectors constitute an overcomplete dictionary, which allow for sparse representations for test pixel vectors as only a few of training vectors are used. Such sparsity can be applied in hyperspectral target detection. However, since the sparse decomposition has the potential instability, similar data often have different estimates. In this letter, we propose a non-local similarity regularized sparsity model to deal with the problem. Non-local similarity enhances classical sparsity model as it preserves the manifold of original data and makes more stable estimations for similar data. In addition, the non-local sparsity model is effectively solved with a developed greedy algorithm. Experimental results suggest an advantage of the non-local sparsity model over conventional sparsity models and a better performance of proposed algorithm compared with conventional sparsity based algorithms.

Index Terms

Hyperspectral Target Detection, Sparse Representation, Non-local Similarity, Greedy Algorithm.

I. Introduction

Hyperspectral imaging sensors produce a three-dimensional (3D) data structure called data cube with two spatial dimensions and one spectral dimension [10]. The spectrum of each hyperspectral pixel can be viewed as a vector with each entry representing the radiance or reflectance value at each spectral band [9], [10]. In hyperspectral imagery (HSI), different materials normally reflect electromagnetic energy at different and specific wavelength bands. Thus when detecting target with specific material, the target pixels are characterized by unique deterministic spectra [9].

The work was supported by the National Natural Science Foundation of China under the Grants 61273245 and 91120301, the 973 Program under the Grant 2010CB327904, the open funding project of State Key Laboratory of Virtual Reality Technology and Systems, Beihang University (Grant No. BUAA-VR-12KF- 07), and Program for New Century Excellent Talents in University of Ministry of Education of China under the Grant NCET-11-0775. The work was also supported by Beijing Key Laboratory of Digital Media, Beihang University, Beijing 100191, P.R. China.

Zhongwei Huang, Zhenwei Shi (corresponding author) and Shuo Yang are with Image Processing Center, School of Astronautics, Beihang University, Beijing, P.R. China, 100191 (E-mails: zhongweiwong@gmail.com; shizhenwei@buaa.edu.cn; yangshuodf@126.com)

So HSI data is suitable for pixel detection with spectral characteristics [10]. The target detection for HSI is a binary classification problem [5] which aims to label each test pixel as target or background. Several detection algorithms have been developed. Most of them are based on statistics [11]. Among them, Adaptive Coherence/Cosine Estimator (ACE) detector, Matched Filter (MF) [11] and Adaptive Subspace Detectors (ASD) [7] are widely used detectors for hyperspectral target detection.

Recently, sparse signal representation has proven to be a powerful tool in many areas [1], [14]. This success is mainly due to the fact that most natural signals can be sparsely represented by a few coefficients carrying the most important information in a certain dictionary or basis set [14]. The nonzero coefficients are critical since they can determine the category of the signal. To apply the sparsity in HSI target detection directly, a pixelwise sparsity model [5] reconstructs and detects each hyperspectral pixel respectively. A joint sparsity model [5] is also proposed for HSI target detection, which assumes the neighboring pixels likely consist of similar materials. So these pixels are sparsely decomposed over an local dictionary simultaneously in joint model. The joint sparsity model suggests a better performance when compared with original pixelwise model.

In contrast to the joint models which consider similarity of data in local areas, we aim to extend it to a non-local fashion. Non-local similarity is believed as an important factor in computer vision and image processing [14], defined as repetitive structures and patterns of data in the whole scene of images [2]. This non-local similarity is effectively applied in image denoising [2] and image restoration [8]. In HSI processing, target pixels are repetitively and irregularly distributed in the whole image. However, conventional sparsity model fails to preserve such non-local similarity [8] which could cause these similar pixels to be decomposed with different sparse coefficients. It will lead to unstable reconstructions and lower detecting performances.

In this letter, we propose a non-local similarity regularized sparsity model for target detection in HSI. The model is based on the idea of capturing and preserving the manifold structure of hyperspectral data. We aim to make a more stable and discriminative sparse representation in which similar signals will obtain similar sparse representations. In proposed model, a constraint is added to preserve the non-local similarity of HSI data. A novel greedy algorithm is proposed for solving the model. Most existing algorithms for effective sparse representation are greedy algorithms [1], [12]. Especially Orthogonal Matching Pursuit (OMP) and Simultaneous Orthogonal Matching Pursuit (SOMP) are used in sparse hyperspectral target detection [5]. We develop the SOMP algorithm in order to effectively solve the proposed model. The proposed algorithm iteratively updates the sub-optimal approximation by solving a Lyapunov Equation [6]. As the accurate solution to such equation is obtained for each iteration, we find an effective solution to the non-local sparsity model.

II. Non-local Similarity based Sparsity Model for HSI Target Detection

In this section, we first review the existing sparsity models for HSI target detection. Then we introduce the non-local similarity regularized sparsity model which aims to improve the detecting performance by enhancing the stability of sparse representation.

A. Current Sparsity Model for Target Detection

If N pixels form an L bands hyperspectral image $\mathbf{X} = \{\mathbf{x}_i\}_{i=1}^{N} \in \mathbb{R}^{L\times N}$, its each pixel $\mathbf{x}_i, i = 1, ..., N$ can be sparsely represented with atoms contains redundant spectral information. Each atom is believed as a training sample that belongs to a particular category, i.e., target or non-target. These atoms constitute an overcomplete spectral dictionary. Denote the spectral dictionary as $\mathbf{D} = [\mathbf{D}_b\ \mathbf{D}_t] \in \mathbb{R}^{L\times M}$, where $\mathbf{D}_b$ and $\mathbf{D}_t$ represents the part of dictionary that respectively containing background and target training samples. Denote $\mathbf{D}_{b_j}, j = 1, ..., M_b$, as columns of $\mathbf{D}_b$ and $\mathbf{D}_{t_j}, j = 1, ..., M_t$, as columns of $\mathbf{D}_t$, where $M = M_b + M_t$. Then any given pixel $\mathbf{x}$ can be written as a linear combination of these training samples:

$$\mathbf{x} = \sum_{j=1}^{M_b} \mathbf{D}_{b_j} s_{b_j} + \sum_{j=1}^{M_t} \mathbf{D}_{t_j} s_{t_j} = \mathbf{D}_b\mathbf{s}_b + \mathbf{D}_t\mathbf{s}_t = \mathbf{D}\mathbf{s}. \tag{1}$$

The coefficients of reconstruction with respectively background and target training samples are denoted with the vector $\mathbf{s} = [\mathbf{s}_b^T\ \mathbf{s}_t^T]^T$.

Suppose the dictionary of training samples $\mathbf{D}$ is redundant, the coefficients vector $\mathbf{s}$ can be very sparse, containing only a few nonzero entries. Given the test pixel $\mathbf{x}$ and training dictionary $\mathbf{D}$, the classical sparsity model for finding coefficients $\mathbf{s}$ is obtained as [1]:

$$(\mathbf{P}_0) : \widehat{\mathbf{s}} = \text{argmin}\|\mathbf{s}\|_0 \quad subject\ to\ \ \mathbf{D}\mathbf{s} = \mathbf{x}. \tag{2}$$

However, a tough issue arises as seeking the optimal solution of $(\mathbf{P}_0)$ is NP-hard [1]. Recent methods all give approximate solvers [1]. Especially, greedy pursuit algorithms [1], [12] provide approximate solutions to a relaxed model with fixed sparsity level K_0:

$$\widehat{\mathbf{s}} = \text{argmin}\|\mathbf{D}\mathbf{s} - \mathbf{x}\|_2 \quad subject\ to\ \ \|\mathbf{s}\|_0 \leq K_0. \tag{3}$$

Once the sparse coefficients $\mathbf{s}$ are obtained, we generate a classifier by incorporating a competition between the target subspace and background subspace. The class of any pixel $\mathbf{x}$ can be determined by:

$$\tilde{d}(\mathbf{x}) = \|\mathbf{x} - \mathbf{D}_b\mathbf{s}_b\|_2 - \|\mathbf{x} - \mathbf{D}_t\mathbf{s}_t\|_2, \tag{4}$$

where $\mathbf{s}_b$ and $\mathbf{s}_t$ respectively represent the recovered sparse coefficients corresponding to the background sub-dictionary $\mathbf{D}_b$ and target sub-dictionary $\mathbf{D}_t$. If $\tilde{d}(\mathbf{x}) > \delta$, where δ is a given threshold, then $\mathbf{x}$ is labeled as a target pixel; otherwise, it is labeled as a background pixel. The nonzero entries of $\mathbf{s}$ are important since they can discriminatively decide whether the test HSI pixel is constructed with background or target training samples.

In addition to pixelwise sparsity model for HSI target detection, a joint sparsity model is proposed [5]. In such model, pixels close to each other in spatial space will be simultaneously reconstructed and detected [5], [13] as pixels in same neighborhood are believed to consist of similar materials.

B. Non-local Similarity Regularized Sparsity Model

In hyperspectral data matrix $\mathbf{X}$, similar spectra representing same materials are repetitively presented. Recent studies have shown the importance of this non-local similarity structure in images [2], [8]. As an unsupervised

learning method, sparse decomposition usually fails to maintain the manifold structure of original data [8]. Especially, in dealing with hyperspectral data, spectra belong to same class may result in different representing coefficients in the sparse reconstruction process. Such undesired condition can be explained by noise or pixel-mixture in hyperspectral scenes. To tackle this problem, we incorporate the assumption that vectors that are similar with each other in the data matrix should have similar sparse representations. In measure such non-local similarity, we use a quadratic constraint with respect to the sparse coefficients:

$$\sum_{i=1}^{N} \|\mathbf{s}_i - \sum_j w_{ji}\mathbf{s}_j\|^2, \tag{5}$$

where $\mathbf{s}_i$ represents the sparse coefficients for a data point $\mathbf{x}_i$ and w_{ji} is the weight parameter representing the similarity between $\mathbf{s}_j$ and $\mathbf{s}_i$. For data matrix $\mathbf{X} = [\mathbf{x}_1 ... \mathbf{x}_N]$, the weight matrix $\mathbf{W} = \{w_{ji}\}_{i,j=1}^{N}$ is obtained by:

$$w_{ji} = e^{-\frac{\|\mathbf{x}_i - \mathbf{x}_j\|^2}{\sigma}}, \tag{6}$$

where σ forces the similarity. When $\mathbf{x}_i$ and $\mathbf{x}_j$ are quite close to each other, w_{ji} will be close to 1 and otherwise we get an output near 0. The constraint in (6) can be transformed by:

$$\begin{aligned} &\sum_{i=1}^{N} \|s_i - \sum_j w_{ji}s_j\|^2 \\ =&\|\mathbf{S} - \mathbf{SW}\|^2 \\ =&Tr(\mathbf{S}(\mathbf{E} - \mathbf{W})(\mathbf{E} - \mathbf{W})^T\mathbf{S}^T) \\ =&Tr(\mathbf{SMS}^T), \end{aligned} \tag{7}$$

where $\mathbf{E}$ is the unit matrix and $\mathbf{M} = (\mathbf{E} - \mathbf{W})(\mathbf{E} - \mathbf{W})^T$.

Similar to (3), for a non-local sparsity model we simultaneously deal with all the test pixels in image $\mathbf{X}$ and the sparse constraint is made on the rows of the coefficient matrix $\mathbf{S} = \{\mathbf{s}_i\}_{i=1}^{N} \in \mathbb{R}^{M \times N}$. Then the problem is defined as:

$$\widehat{\mathbf{S}} = \text{argmin}\|\mathbf{DS} - \mathbf{X}\|_F \quad subject\ to\ \ \|\mathbf{S}\|_{row,0} \leq K_0, \tag{8}$$

where $\|\cdot\|_F$ denotes the Frobenius norm. In proposed method, this term is regularized for computational convenience. When add the constraint in (7) into (8), we obtain the following optimization problem:

$$\begin{aligned} \widehat{\mathbf{S}} =&\text{argmin}\frac{1}{2}\|\mathbf{DS} - \mathbf{X}\|_F^2 + \lambda Tr(\mathbf{SMS}^T) \\ &subject\ to\ \ \|\mathbf{S}\|_{row,0} \leq K_0, \end{aligned} \tag{9}$$

where λ is a regularization parameter controlling the level of the non-local similarity constraint.

III. Non-local Similarity based SOMP

In proposed method, (9) is solved with a greedy algorithm based on conventional Simultaneous Orthogonal Matching Pursuit (SOMP) [4]. As our method incorporates the non-local similarity constraint, we denote the proposed algorithm as Non-local Similarity based SOMP (NS-SOMP).

The greedy algorithms are believed to be efficient for sparse representation [1], [12]. Generally, greedy algorithms search exhaustively in each iteration to find a sub-optimal approximation, by picking the vector that best correlates with the present residual. Recent studies have reported the good performances of greedy algorithms especially SOMP in dealing with hyperspectral target detection [5]. In each iteration of the SOMP algorithm for solving (3), the index of one atom within $\mathbf{D}$ is picked if it most close to the current residuals $\mathbf{R}$. Then current index set Λ_k is updated by add this index to it. Then a sub-optimal solution denoted as $\mathbf{P}_k$ is obtained using atoms within the index set which is denoted as $\mathbf{D}_{\Lambda_k}$ and the residuals is updated with the solution. When stopping criterion is met, the sparse representation is obtained using atoms within the final index set Λ approximately by:

$$\widehat{\mathbf{S}} = (\mathbf{D}_{\Lambda}^T\mathbf{D}_{\Lambda}^T)^{-1}\mathbf{D}_{\Lambda}^T\mathbf{X}. \tag{10}$$

To solve the optimization problem in (9) with the greedy algorithm, we first attempt to find an accurate sub-optimal solution for each iteration, i.e., we aim to solve the unconstrained problem in kth iteration:

$$\widehat{\mathbf{P}}_k = \text{argmin}\frac{1}{2}\|\mathbf{D}_{\Lambda_k}\mathbf{P}_k - \mathbf{X}\|_F^2 + \lambda Tr(\mathbf{P}_k\mathbf{M}\mathbf{P}_k^T). \tag{11}$$

The gradient of $f_{(\mathbf{P}_k)} = \frac{1}{2}\|\mathbf{D}_{\Lambda_k}\mathbf{P}_k - \mathbf{X}\|_F^2 + \lambda Tr(\mathbf{P}_k\mathbf{M}\mathbf{P}_k^T)$ can be obtained as:

$$\nabla f_{(\mathbf{P}_k)} = \mathbf{D}_{\Lambda_k}^T\mathbf{D}_{\Lambda_k}\mathbf{P}_k - \mathbf{D}_{\Lambda_k}^T\mathbf{X} + \lambda\mathbf{P}_k(\mathbf{M} + \mathbf{M}^T). \tag{12}$$

When forcing the gradient to be zero, we obtain an equation:

$$\mathbf{D}_{\Lambda_k}^T\mathbf{D}_{\Lambda_k}\mathbf{P}_k - \mathbf{D}_{\Lambda_k}^T\mathbf{X} + \lambda\mathbf{P}_k(\mathbf{M} + \mathbf{M}^T) = 0, \tag{13}$$

which is actually a Lyapunov Equation [6]. Donate $\mathbf{A} = \mathbf{D}_{\Lambda_k}^T\mathbf{D}_{\Lambda_k}$,$\mathbf{B} = \lambda(\mathbf{M} + \mathbf{M}^T)$, $\mathbf{C} = \mathbf{D}_{\Lambda_k}^T\mathbf{X}$, the Lyapunov Equation is obtained as:

$$\mathbf{A}\mathbf{P}_k + \mathbf{P}_k\mathbf{B} = \mathbf{C}. \tag{14}$$

Its solution is normally obtained as:

$$vec(\mathbf{P}_k) = (\mathbf{E} \otimes \mathbf{A} + \mathbf{B}^T \otimes \mathbf{E})^{-1}vec(\mathbf{C}), \tag{15}$$

where $\mathbf{E}$ still denotes the unite matrix and vec reshape a matrix column-wise to a vector. The Kronecker product [6] is denoted with $\otimes$. However the Kronecker product calls heavy consumption for memory, so in most cases when matrix $\mathbf{A}$ and $\mathbf{B}$ can be diagonalized , we use the method proposed in [6]. The eigenvalue decompositions of matrix $\mathbf{A}$ and $\mathbf{B}$ are respectively obtained as:

$$\mathbf{U}^{-1}\mathbf{A}\mathbf{U} = \begin{bmatrix} \alpha_1 & & \\ & \ddots & \\ & & \alpha_M \end{bmatrix}, \mathbf{V}^{-1}\mathbf{B}\mathbf{V} = \begin{bmatrix} \beta_1 & & \\ & \ddots & \\ & & \beta_N \end{bmatrix}. \tag{16}$$

Then the solution $\mathbf{P}_k$ is obtained by:

$$\mathbf{P}_k = \mathbf{U}\tilde{\mathbf{P}}_k\mathbf{V}^{-1}, \tag{17}$$

where $\tilde{\mathbf{P}}_{k_{ij}} = \frac{\tilde{\mathbf{C}}_{ij}}{\alpha_i+\beta_j}$, $i = 1, ..., M$, $j = 1, ..., N$ and $\tilde{\mathbf{C}} = \mathbf{U}^{-1}\mathbf{C}\mathbf{V}$. Then we apply the above-mentioned method to update the sub-optimal solution in each iteration of SOMP. The outline of proposed algorithm NS-SOMP is given below:

Algorithm 1 Pseudocode of the NS-SOMP Algorithm.

1: **Input**:

$L \times M$ dictionary $\mathbf{D} = [\mathbf{d}_1 \cdots \mathbf{d}_M]$, $L \times N$ data matrix $\mathbf{X} = [\mathbf{x}_1 \cdots \mathbf{x}_N]$, similarity matrix $\mathbf{M}$, a stopping criterion.

2: Initialization:

iteration: $k = 1$,

initial index set: $\Lambda_0 = \emptyset$,

initial residual: $\mathbf{R}_0 = \mathbf{X}$.

3: Main iteration:

Find the index of atoms that most close to residuals:

$index \Leftarrow arg\min_{1 \le i \le M} \|\mathbf{d}_i^T \mathbf{R}_{k-1}\|_2$

Update the index set: $\Lambda_k \Leftarrow \Lambda_{k-1} \cup \{index\}$

Compute $\mathbf{P}_k$ with solving the Layapunov Equation:

$\mathbf{P}_k \in \mathbb{R}^{k \times N} \Leftarrow \mathbf{D}_{\Lambda_k}^T \mathbf{D}_{\Lambda_k} \mathbf{P}_k - \mathbf{D}_{\Lambda_k}^T \mathbf{X} + \lambda \mathbf{P}_k (\mathbf{M} + \mathbf{M}^T) = 0$

Update residual: $\mathbf{R}_k \Leftarrow \mathbf{X} - \mathbf{D}_{\Lambda_k} \mathbf{P}_k$

Update iteration: $k \Leftarrow k + 1$

4: Stop if criterion has been met. Otherwise, repeat another iteration.

5: **Output**:

final index set $\Lambda = \Lambda_{k-1}$,

sparse representation $\widehat{\mathbf{S}} = (\mathbf{D}_\Lambda^T \mathbf{D}_\Lambda^T)^{-1} \mathbf{D}_\Lambda^T \mathbf{X}$.

Once the sparse representation matrix $\widehat{\mathbf{S}}$ is obtained, we could label the pixels in the whole image with the classifier we have introduced in (4).

In order to illustrate the advancement of proposed model and algorithm on sparse reconstruction, we compare it with conventional pixel-wise SOMP on six hyperspectral pixels. The reconstruction results are compared in Fig. 1(a)-(c). The test pixels are randomly extracted from the background pixels in three different positions in the real hyperspectral data displayed in Fig. 2(a). The experiments on the data will be fully explained in section IV. In order to illustrate the efficiency of proposed method, we compare the SOMP and NS-SOMP algorithm under the same condition and it can be seen that the reconstructed data is closer to the original data with constraint of non-local similarity. The relative construction error is also computed as shown in Table 1. For a test pixel $\mathbf{x}$, a given spectral dictionary $\mathbf{D}$ and the sparse coefficients $\mathbf{s}$ obtained, we evaluate the construction with a relative error $e(\mathbf{x}) = \frac{\|\mathbf{D}\mathbf{s}-\mathbf{x}\|_2}{\|\mathbf{x}\|_2}$. As a better reconstruction will result in a smaller error, the non-local similarity constraint enhances the accuracy and stability of the sparse representation in general.

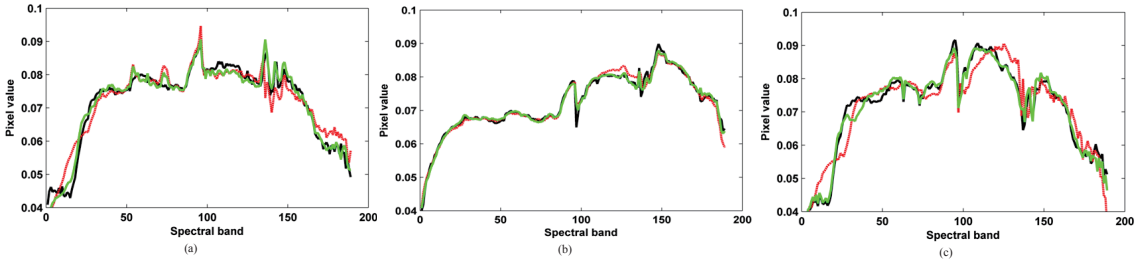

Fig. 1. Sparse reconstruction examples for hyperpspectral data (black) with two algorithms SOMP (red) and NS-SOMP (green). For comparison, the reconstructions with the two algorithms are applied with same sparsity $K_0 = 5$ and based on the same dictionary.

Error (in percentage)	a	b	c
SOMP	5.29	2.05	6.41
NS-SOMP	2.82	1.34	2.61

TABLE I

THE RELATIVE ERROR OF THE RECONSTRUCTION PROVIDED BY SOMP AND NS-SOMP ARE COMPUTED AND SHOWN IN PERCENTAGES.

IV. EXPERIMENTAL RESULTS

In this section, we use two real hyperspectral images to demonstrate the efficiency of non-local similarity based sparsity model. In the experiments, the proposed NS-SOMP algorithm is compared with the joint sparsity algorithm [5], pixelwise greedy algorithms SOMP, OMP [13] and three statistics based algorithms Adaptive Coherence/Cosine Estimator (ACE) detector, Matched Filter (MF) [11] and Adaptive Subspace Detectors (ASD) [7]. The results of these algorithms are evaluated both visually and quantitatively by the receiver operating characteristics (ROC) curves [3]. The ROC curve is a graphical plot which illustrates the performance of a detector. As the threshold varying in the whole possible region, the ROC curve is generated by plotting PD (probability of detection) as a function of PFA (probability of false alarms). PD is calculated by the ratio of the number of target pixels that are labeled as targets and the total number of true target pixels. While PFA is calculated by the ratio of the number of background pixels that are labeled as targets and the total number of pixels. ROC analysis provides tools to compare detectors quantitatively, i.e., the lager the area embraced by the plot, the better the detector performs.

In our experiments, the real hyperspectral images are collected by the Airborne Visible/Infrared Imaging Spectrometer (AVIRIS) sensor. The scenes are two parts of the airport in San Diego, America. The AVIRIS sensor collects the spectral data in 224 bands, and the spectral range is 0.4-2.5μm. We have removed the water absorption and low SNR bands, and 189 available bands were left. There are two kinds of airplanes which are detected as targets in two separated images, namely AVIRIS-I with size of 100×100 pixels and AVIRIS-II with size of 200×200 pixels. The first kind of three airplanes locates in the upper left corner of the image, shown in Fig. 2(a). The second kind of three airplanes locates in the lower right corner of the image, shown in Fig. 3(a). For these two images,

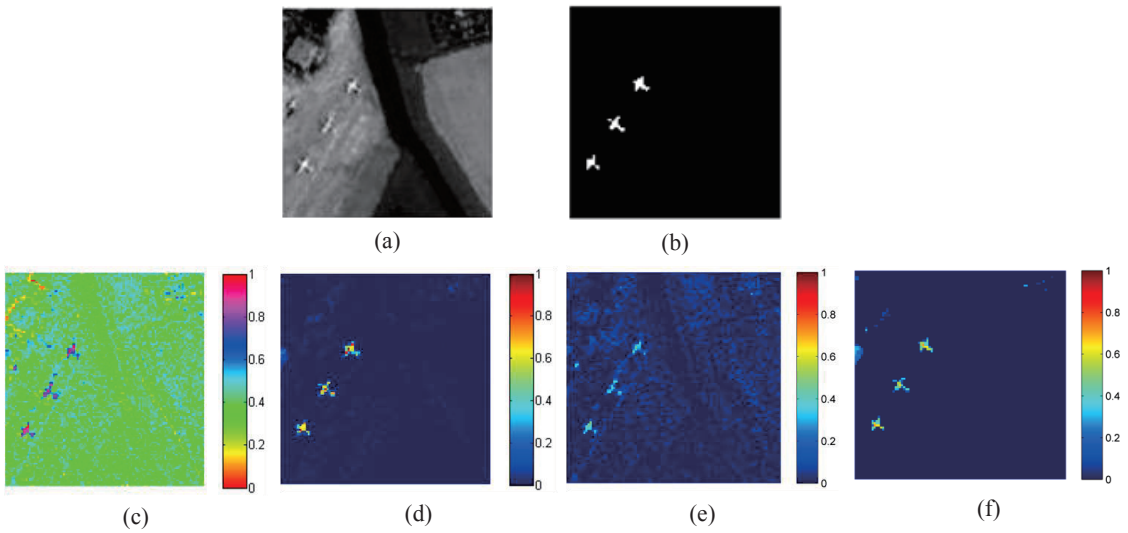

Fig. 2. AVIRIS-I. (a) First band of original hyperspectral data. (b) Ground truth of AVIRIS-I. Detection results for AVIRIS-I with (c) MF (d) ACE (e) J-SOMP (f) NS-SOMP.

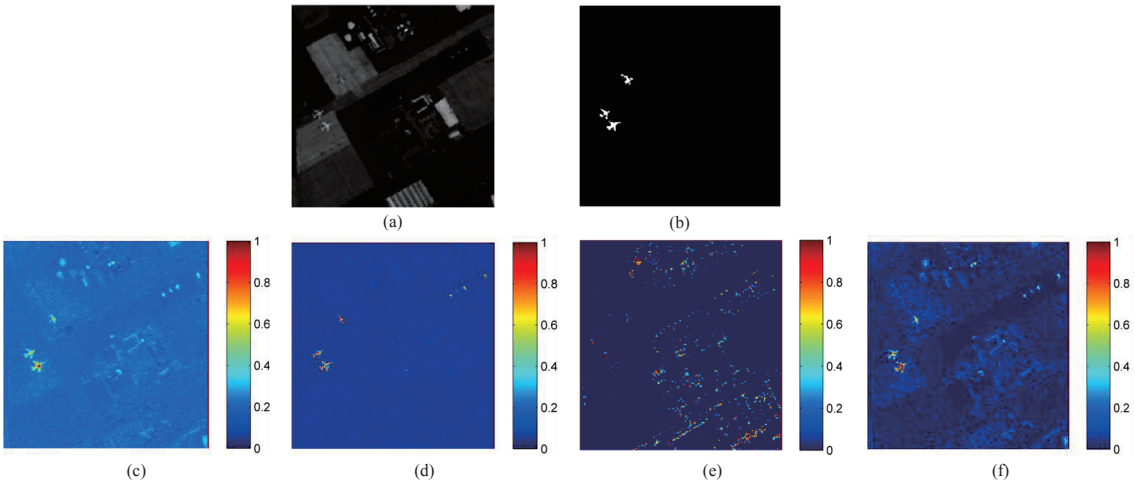

Fig. 3. AVIRIS-II. (a) First band of original hyperspectral data. (b) Ground truth of AVIRIS-II. Detection results for AVIRIS-I with (c) MF (d) ACE (e) J-SOMP (f) NS-SOMP.

each pixel on the targets is considered as a target pixel.

For sparsity-based algorithms, the spectral dictionary $\mathbf{D}$ is constructed with two parts: the background sub-dictionary $\mathbf{D}_b$ and the target sub-dictionary $\mathbf{D}_t$. For the joint sparsity model used in our experiments, the target sub-dictionary $\mathbf{D}_t$ is generated by K-means clustering with target pixels and the number of the cluster centers is set to be 10, as described in [4]. Thus the target dictionary consists of 10 atoms in all. We use the dual window

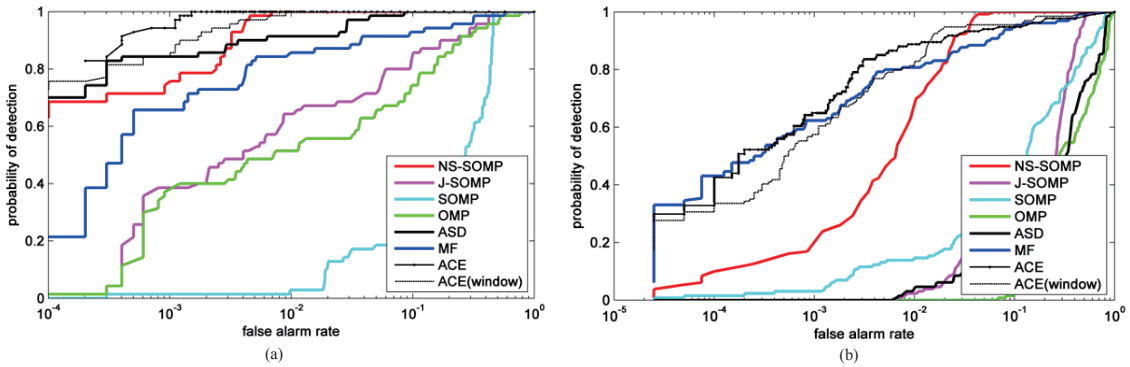

Fig. 4. ROC curves for AVIRIS-I in (a) and for AVIRIS-II in (b) with respectively eight different detection algorithms: NS-SOMP, J-SOMP, SOMP, OMP, ASD, MF, ACE and sliding window version of ACE.

approach [4] to generate the background sub-dictionary for the joint sparsity model [5]. The size of inner windows is set to be 15×15 which is most close to the size of each plane [4] and the size of outer windows is set to be 25×25, thus each background dictionary contains 400 atoms in all. The joint sparsity model is solved with SOMP [5] and denoted as J-SOMP in our experiments. For the non-local similarity and pixelwise sparsity model based algorithms, $\mathbf{D}_t$ is the prior knowledge of one spectrum of the targets. Also, a non-local background dictionary $\mathbf{D}_b$ is respectively constructed using K-means clustering. The background pixels are clustered into 400 atoms in the background dictionary $\mathbf{D}_b$.

Instead of J-SOMP, all other algorithms in our experiments use the same target of spectrum for detection. Especially in ASD, it is used to generate the target subspace [7]. The outputs of detectors based on MF, ACE, joint and non-local similarity based sparsity model for AVIRIS-I are shown in Fig.2(c)-(f) respectively and their output for AVIRIS-II are shown in Fig. 3(c)-(f) respectively. The outputs are all converted to grayscale images and displayed with false color plots. The color scale bar for each plot are also provided. The ROC curves for AVIRIS-I and AVIRIS-II are displayed in Fig. 4(a) and (b) respectively with eight different detection algorithms: NS-SOMP, J-SOMP, SOMP, OMP, ASD, MF, ACE and a sliding window version of ACE. We generate the sliding window version of ACE using the same dual window approach as J-SOMP does. For AVIRIS-I and AVIRIS-II we use the same sparsity $K_0 = 10$ for all the sparsity based algorithms as the stopping criterion. The parameter σ for similarity constraint in NS-SOMP is set to be 1. The performance of most detectors on AVIRIS-I suggest a good performance. Among the sparsity based algorithms, NS-SOMP performs the best and J-SOMP also suggests an advantage over pixelwise sparse detectors. Statistics based algorithms outperforms sparsity based algorithms and ACE gets the best performance. This is mainly because the scene is relatively small and simple.

In the ROC curves for AVIRIS-II, it can be illustrated that most sparse detectors fail to detect the three planes well. This is because the scene is more complex and could lead to unstable sparse reconstructions. Especially joint sparsity model fails to perform well since the dual window approach may not constitute a qualified background dictionary.

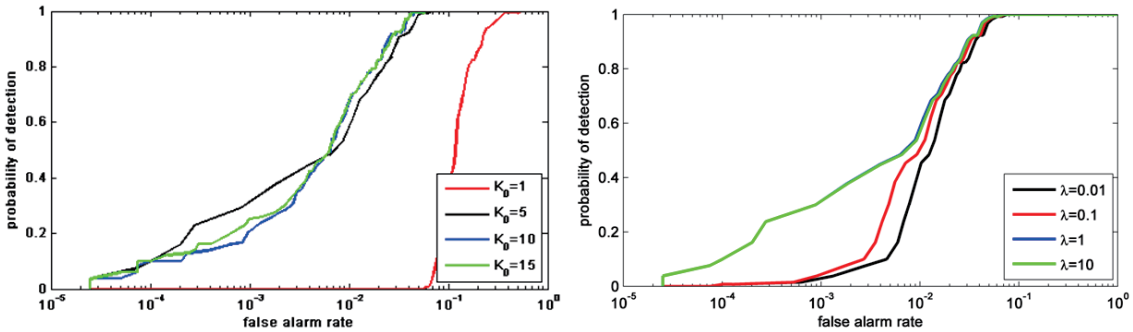

Fig. 5. ROC curves for AVIRIS-II using NS-SOMP with different level of sparsity K_0 in (a) and different level of constraint on non-local similarity λ in (b).

In addition, the local similarity can be not effectively applicable under complex conditions. Thus conventional sparsity model can not guarantee an accurate representation especially for the targets. The proposed NS-SOMP detection algorithm is the only sparse method that have good performance for AVIRIS-II, whose ROC curve is higher and more quickly reached to 1 compared with other sparsity based algorithms. Compared with ACE and MF, the proposed NS-SOMP falls behind at low false alarm rate but suggests a better performance at high false alarm rate. Such result suggests that in occasions that we could not afford loss of any targets, the proposed NS-SOMP will become a better alternative to conventional methods.

We also demonstrate the effects of two important factors in NS-SOMP algorithm, i.e., the sparsity K_0 and the similarity constraint parameter λ in (9). We test the performance of proposed NS-SOMP on AVIRIS-II with different levels of these two parameters and display the ROC curves as shown in Fig. 5(a) and (b). ROC curves in Fig. 5(a) suggest a ascending performance with increased sparsity K_0 from 1 to 10 and λ is fixed at 1 in this experiment. The ROC curves in Fig. 5(b) suggest the importance of incorporating the non-local similarity constraint and the sparsity K_0 is fixed at 10 in this experiment. The performance is also greater with stronger constraint in an appropriate range from $\lambda = 0.01$ to $\lambda = 1$ and the curves representing $\lambda = 1$ and $\lambda = 10$ coincide with each other.

V. Conclusion

In this letter, we have proposed a non-local similarity regularized sparsity model for hyperspectral target detection. The model is solved with a novel algorithm called the non-local similarity based SOMP (NS-SOMP). The sparse representation is believed to be unstable in conventional approaches. As non-local similarity contains the important manifold structure of the original data, such information is effectively applied in our sparsity model to enhance the stability of sparse representation. Experiments on real hyperspectral data suggest the advancement of proposed model over existing pixelwise and joint sparsity model. The proposed detection algorithm NS-SOMP also has a better performance than conventional sparse algorithms.

REFERENCES

[1] A. M. Bruckstein, D. L. Donoho and Michael Elad, "From sparse solutions of systems of equations to sparse modeling of signals and images," Siam Review, Society for Industrial and Applied Mathematics, vol. 51, no. 1, pp. 34-81, 2009.

[2] A. Buades, B. Coll, and J. Morel, "A non-local algorithm for image denoisng," In Proceedings of IEEE Conference on Computer Vision and Pattern Recognition, vol. 2, pp. 60-65, 2005.

[3] C. I. Chang, "Multiparameter receiver operating characteristic analysis for signal detection and classification," IEEE Sensors J., vol. 10, no. 3, pp. 423-442, Mar. 2010.

[4] Y. Chen, N. M. Nasrabadi, and T. D. Tran, "Sparse representation for target detection in hyperspectral imagery," IEEE J. Sel. Topics Signal Process., vol. 5, no. 3, pp. 629-640, 2010.

[5] Yi Chen, N. M. Nasrabadi, T. D. Tran, "Simultaneous joint sparsity model for target detection in hyperspectral imagery," IEEE Geosci. Remote Sens. Lett., vol. 8, no. 4, pp. 676-680, Jul. 2011.

[6] A. Jameson, "Solution of the equation AX + XA = C by inversion of an M $\times$ M or N $\times$ N matrix," SIAM J. Appl. Math., vol. 16, pp. 1020-1023, 1968.

[7] S. Kraut, L.L. Scharf, and L.T. McWhorter, "Adaptive subspace detectors," IEEE Trans. Signal Processing, vol. 49, no. 1, pp. 1-16, Jan. 2001.

[8] J. Mairal, F. Bach, J. Ponce, G. Sapiro, and A. zisserman, "Non-local sparse models for image restoration," In Proceed- ings of IEEE International Conference Computer Vision, pp. 2272-2279, 2009.

[9] D.Manolakis and G. Shaw, "Detection algorithms for hyperspectral imaging applications," IEEE Signal Process. Mag., vol. 19, no. 1, pp. 29-43, Jan. 2002.

[10] D. Manolakis, D. Marden, G. A. Shaw, "Hyperspectral image processing for automatic target detection applications," Lincoln Laboratory Journal, vol. 34, no. 1 pp. 79-116, 2003.

[11] D. Manolakis, R. Lockwood, T. Cooley, J. Jacobson, "Is there a best hyperspectral detection algorithm?," Algorithms Technol. Multispectral, Hyperspectral, Ultraspectral Imagery XV, vol. 7334, no. 1, pp. 733402-1-733402-16, 2009.

[12] J. A. Tropp, "Greed is good: Algorithmic results for sparse approximation," IEEE Trans. Inf. Theory, vol. 50, no. 10, pp. 2231-2242, Oct. 2004.

[13] J. A. Tropp, A. C. Gilbert, and M. J. Strauss, "Algorithms for simultaneous sparse approximation. Part I: Greedy pursuit," Signal Process. Special Issue on Sparse Approximations in Signal and Image Processing, vol. 86, no. 3, pp. 572-588, Mar. 2006.

[14] J. Wright, Y. Ma, J. Mairal, G. Sapiro, T. Huang, and S. Yan, "Sparse representation for computer vision and pattern recognition," Proc. IEEE, vol. 98, no. 6, pp. 1031-1044, Jun. 2010.